J. Membrane Biol. 109, 9–19 (1989)

The Journal of
Membrane Biology

Current-Voltage Relationships of a Sodium-Sensitive Potassium Channel in the Tonoplast of *Chara corallina*

Adam Bertl*
Pflanzenphysiologisches Institut und Botanischer Garten der Universität Göttingen, D-3400 Göttingen, Federal Republic of Germany

Summary. The membrane of mechanically prepared vesicles of *Chara corallina* has been investigated by patch-clamp techniques. This membrane consists of tonoplast as demonstrated by the measurement of ATP-driven currents directed into the vesicles as well as by the ATP-dependent accumulation of neutral red. Addition of 1 mM ATP to the bath medium induced a membrane current of about 3.2 mA · m^{-2} creating a voltage across the tonoplast of about −7 mV (cytoplasmic side negative). On excised tonoplast patches, currents through single K^+-selective channels have been investigated under various ionic conditions. The open-channel currents saturate at large voltage displacements from the equilibrium voltage for K^+ with limiting currents of about +15 and −30 pA, respectively, as measured in symmetric 250 mM KCl solutions. The channel is virtually impermeable to Na^+ and Cl^-. However, addition of Na^+ decreases the K^+ currents. The *I-V* relationships of the open channel as measured at various K^+ concentrations with or without Na^+ added are described by a 6-state model, the 12 parameters of which are determined to fit the experimental data.

Key Words *Chara corallina* · tonoplast · K^+ channel · Na^+ effect · cyclic model

Introduction

As far as plant membranes are concerned, the macroscopic electrical properties are rather well investigated for the plasmalemma of giant algal cells of the *Characeae* (for reviews *see* Hope & Walker, 1975; Beilby, 1985). On the other hand, the knowledge about the electrical properties of the tonoplast even in these cells has lagged far behind until recently. This delay can be ascribed to the inaccessibility of the tonoplast in intact cells and the difficulties in changing the ionic composition on each side of the membrane.

Electrophysiological access to the tonoplast of *Chara* has been gained by the application of the vacuolar perfusion technique (Tazawa, Kikuyama & Shimmen, 1976) as well as by the use of permeabilized cells (Shimmen & Tazawa, 1983). The vacuolar perfusion technique provides the opportunity to study the electrical characteristics of the tonoplast while being able to control the ionic conditions at the vacuolar side of the membrane by replacement of the vacuolar sap by an artificial solution (Tazawa et al., 1976). In permeabilized cells, where the plasmalemma of the cells is made irreversibly and highly permeable to small molecules and ions, the electrical characteristics of the tonoplast can be investigated under known ionic conditions at the cytoplasmic side of the membrane (Tester, Beilby & Shimmen, 1987). In addition to the control of the ionic conditions on both sides of the membrane, patch-clamp techniques (for a collection of fundamental contributions in this field, *see* Sakmann & Neher, 1983) provide the possibility of investigating ion transport mechanisms on the level of individual ion transporters.

Recently, in a patch-clamp survey of ion channels and proton pumps, Hedrich et al. (1988) postulated that in plant cells the efflux of anions from the vacuole and the equilibrium of cations across the tonoplast is mediated by a channel of low selectivity.

In contrast to this unspecific channel described for the tonoplast of various higher plant cells (Hedrich, Flügge & Fernandez, 1986; Coyaud et al., 1987; Hedrich & Neher, 1987; Hedrich et al., 1988), a K^+-selective channel was demonstrated to be the predominant channel in the outer membrane of cytoplasmic droplets of *Chara corallina* (Lühring, 1986; Laver & Walker, 1987). However, it is still a matter of discussion whether the enclosing membrane consists of (inverse) tonoplast (Reeves, Shim-

* *Present address:* Department of Cellular and Molecular Physiology, Yale University, School of Medicine, 333 Cedar Street, New Haven, CT 06510.

men & Tazawa, 1985; Lühring, 1986; Sakano & Tazawa, 1986; Laver & Walker, 1987) or of plasmalemma (Svintitskikh, Andrionov & Bulychev, 1985; Homble, Ferrier & Dainty, 1987).

The aim of this study is to gain unambiguous information about the origin of these channels. The major subject, however, is to determine the parameters of the catalytic reaction cycle of this K^+ translocating enzyme including the inhibitory role of Na^+.

Materials and Methods

Isolation of Tonoplast Vesicles

For isolation of tonoplast vesicles an internodal cell of *Chara corallina* was incubated for about 10–20 sec in 1 M NaCl, placed on an inclined glass disk and cut off at both ends with fine scissors. The cell content was swept out into the measuring chamber by perfusion of the cell with the standard bath solution, which contained 250 mM KCl and 1 mM $CaCl_2$ adjusted to pH 7 by about 5 mM Tris/MES. In this solution transparent vesicles (never containing chloroplasts) with diameters of 5–200 μm could be found.

Patch-Clamp Experiments

Patch-clamp experiments were carried out according to the methods described by Hamill et al. (1981). Throughout the records, voltages are given as cytoplasmic potential minus extraplasmic (vacuolar) potential. Correspondingly, the flow of positive charges directed from the cytoplasmic side to the vacuolar side (or negative charges in the opposite direction) is a positive current and defined as an outward current.

In excised membrane patches, single-channel currents were measured over a voltage range of up to ±200 mV at various salt concentrations, as indicated in the inset of the respective figure. All solutions contained 1 mM $CaCl_2$ and were buffered by about 5 mM Tris/MES adjusted to pH 7–7.2 (in the experiment of Fig. 6*B*, where Na^+ has been added as NaOH, the pH has been adjusted by MES, assuming MES does not affect the currents).

The current records were digitized by a modified digital audio processor (PCM-501ES, Sony, Japan) and stored on a video recorder (VS220 RC, Grundig, FRG). For data analysis, the records were played back to a digital oscilloscope (2090-3 Nicolet) and copied by an *x-y* plotter (Gila 2000, Laumann, FRG). The current amplitudes were evaluated by hand.

Results

Neutral Red Accumulation

The existence of an ATP-dependent H^+-pump in the tonoplast of *Chara corallina* (Moriyasu, Shimmen & Tazawa, 1984) can be used for identification of intact tonoplast.

All vesicles, prepared as described above, were red in the standard bath solution, when isolated after staining the vacuole of an intact internodal cell by incubation of the cell for 1 hr in natural pond water with 0.1 mM neutral red. This observation indicates the vesicles contained vacuolar sap and maintained a pH gradient during the isolation procedure.

Vesicles prepared from unstained internodal cells turned red upon addition of 1 mM Mg-ATP and 25 μM neutral red (*not shown*), indicating an ATP-driven acidification of the vesicles.

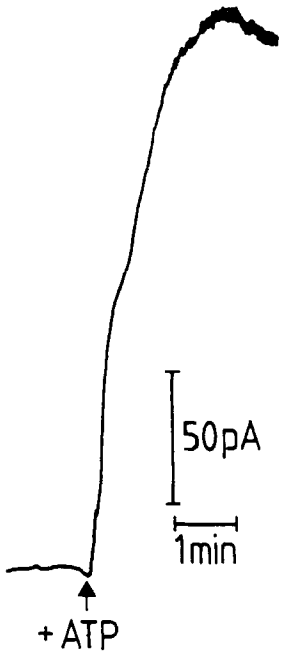

Fig. 1. ATP-driven current from a tonoplast vesicle of *Chara corallina* (100 μm in diameter) recorded in the 'whole-vesicle' mode (according to whole-cell). Positive currents (upward deflection) are currents from the cytoplasmic side into the vesicle. Solutions in pipette and bath were 250 mM NaCl, 1 mM $CaCl_2$ adjusted to pH 7. Addition of 1 mM Mg-ATP as indicated by the arrow

ATP-Driven Currents

ATP-driven currents have been measured directly by means of whole vesicle recordings. In the voltage-clamp mode, with the membrane clamped at 0 mV, the application of 1 mM Mg-ATP to the bath (cytoplasmic side) caused a current of some 100 pA directed into the vesicle. For a tonoplast vesicle with a diameter of 100 μm, as in the example of Fig. 1, the total ATP-driven current corresponds to a membrane current of 3.2 $mA \cdot m^{-2}$. Under the given experimental conditions (*see* legend to Fig. 1), this current results in a hyperpolarization of the

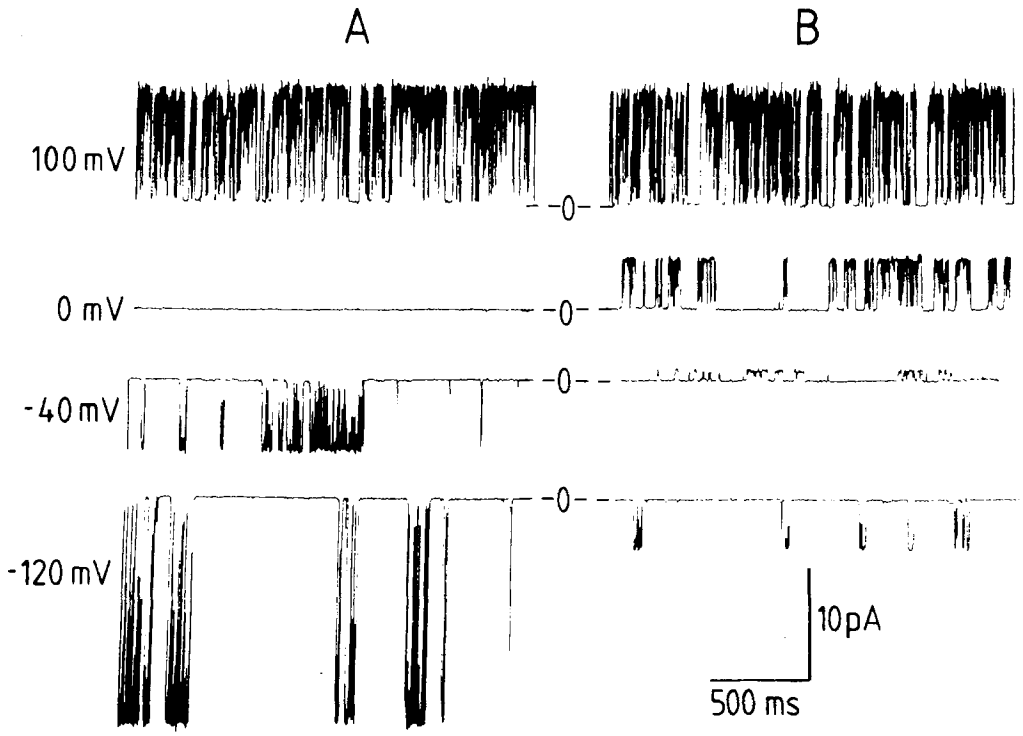

Fig. 2. Examples of single-channel currents at various membrane voltages (cytoplasmic side *vs.* vacuolar side) recorded on excised membrane patches. Vacuolar K^+ concentration was 250 mM in *A*, and 25 mM in *B*; cytoplasmic K^+ was 250 mM throughout. Membrane voltages are given on the left of each record; – –0– – marks the baseline of each record, i.e., the current with the channel closed. Upward deflections are positive currents directed from the cytoplasmic side to the vacuolar side. The seal resistance was 30 GΩ in *A* and 25 GΩ in *B*. Signals were low-pass filtered at 1 kHz

tonoplast from 0 to −7 mV (cytoplasmic side being negative), as measured by briefly switching from the voltage-clamp mode to the current-clamp mode when the ATP-induced current reached its maximum.

Current-Voltage Relationships of the Open-Channel Currents

Figure 2 shows some examples of these single-channel current recordings in symmetrical 250 mM KCl (Fig. 2*A*) and under asymmetrical conditions with 250 mM KCl at the cytoplasmic side of the membrane and 25 mM KCl at the vacuolar side (Fig. 2*B*). In this figure, the actual membrane voltage (*see* definition in Materials and Methods) is given at the left, made for the corresponding traces in experiments *A* and *B*. The baseline is marked by "-0-", indicating the current through the membrane patch with the channel being closed. Deviations from this baseline are currents through the channel, where upward deflections are positive currents, downward deflections are negative ones.

The steady-state current-voltage (*I-V*) relationships of the open channel have been found to provide the experimental information for the determination of the catalytic reaction cycle of ion transport (Gradmann et al., 1987). In Figs. 3-8, the experimental data are given by points. The curves in these figures are fitted curves, which are the subject of the discussion following.

Changes of the Vacuolar K^+ Concentration

Figure 3 displays a set of *I-V* relationships for a cytoplasmic KCl concentration of 250 mM and vacuolar KCl concentrations ranging from 2.5 to 250 mM. The data in this figure reveal some important features of the channel.

In symmetrical solutions with 250 mM KCl at both sides of the membrane (Fig. 3*A*) the *I-V* relationship is asymmetric with respect to the current amplitudes. At large voltage displacements, negative currents are about twice the positive ones.

Variation of the vacuolar KCl concentration leads to reversal voltages close to the respective equilibrium voltage for K^+ as calculated by the Nernst equation using the K^+ activities (ionic activities have been calculated by the "Debye-Hückel

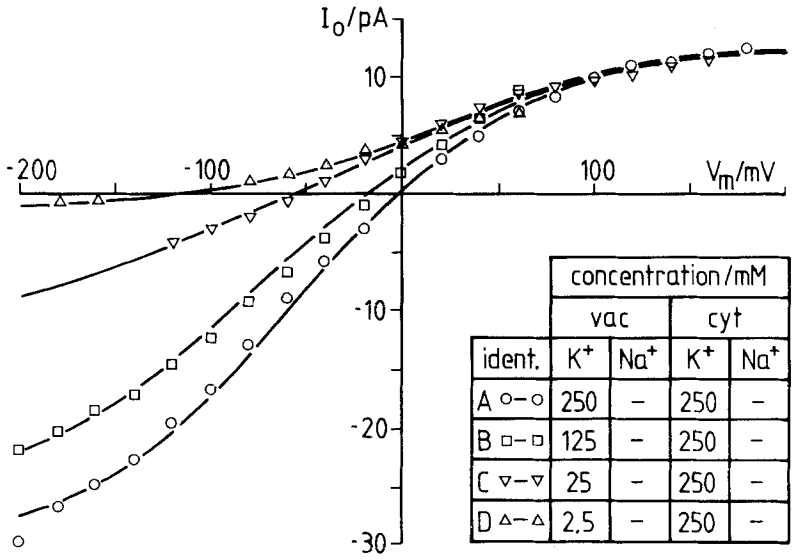

Fig. 3. Current-voltage relationships of the open channel as a function of external (vacuolar) K^+ concentrations obtained from single-channel recordings from excised membrane patches. Data (points) are from four different experiments. Ionic conditions are as indicated in the inset. Decreasing K^+ has been compensated by mannitol or sorbitol. Curves: fits of Eq. (10) to the data with the parameters of the 6-state model are given in Table 3

Table 1. Equilibrium voltages for K^+ as calculated by the Nernst equation using the respective K^+ activities (not the concentrations) and reversal voltages measured by the experiments to Fig. 3[a]

Curve	$[K^+]_o$/mM	$[K^+]_i$/mM	E_{K^+}/mV (calc)	E_{K^+}/mV (meas)
A	185	185	0	0
B	99	185	−16	−16
C	22	185	−54	−55
D	2.4	185	−111	−117

[a] Ion-activities have been calculated by the "Debye-Hückel limiting law."

limiting law"). Therefore the currents are K^+ currents. Measured reversal voltages as well as the calculated equilibrium voltages for K^+ are listed in Table 1.

Further, it can be seen from Fig. 3*A-D* that the open-channel currents tend to saturate at large voltage displacements. Clear saturation can be seen for positive currents and at least a tendency toward saturation for negative currents.

The positive saturation current appears to be insensitive to changes of the vacuolar K^+ concentration. The saturation characteristic of the negative currents apparently depends on the vacuolar K^+, but in a subproportional manner.

Replacement of K^+ by Na^+

Upon replacement of K^+ by Na^+ at the vacuolar side (Fig. 4*B*), the positive saturation current remained almost the same as in the control with 250 mM KCl at both sides of the membrane (Fig. 4*A*, reproduced from Fig. 3*A*) but the *I-V* relationship flattened. The positive currents vanished with increasing negative voltages and no negative currents could be detected not even at −200 mV (i.e., no finite reversal voltage could be determined). Vice versa, no positive currents could be measured when K^+ was replaced by Na^+ at the cytoplasmic side (Fig. 4*C*).

Effect of Na^+ on K^+ Currents

Figure 5*A* displays the *I-V* relationship at 125 mM vacuolar and 250 mM cytoplasmic KCl (reproduced from Fig. 3*B*). Addition of 125 mM NaCl at the vacuolar side of the membrane while maintaining the KCl concentration at 125 mM (Fig. 5*B*) resulted in smaller negative currents, while the reversal voltage as well as the positive saturation current remained almost unaffected. These phenomena can also be observed in Fig. 5*C* and *D*, at vacuolar concentrations of 25 mM KCl in the control (*C*) and 25 mM KCl plus 225 mM NaCl in *D*. At the cytoplasmic side the solutions contained 250 mM KCl throughout the experiments of Fig. 5. The small shift of the reversal voltages towards more negative values in data *B* compared to *A* and in *D* compared to *C* correspond to a decrease of the K^+ activities when the total salt concentration is increased.

The data in Fig. 6 show the *I-V* relationships of the open channel in the presence of 125 mM K^+ plus 125 mM Na^+ and either 250 mM Cl^- (*A* reproduced from Fig. 5*B*) or 125 mM Cl^- (*B*) at the vacuolar side. Cytoplasmic salt concentration was 250 mM

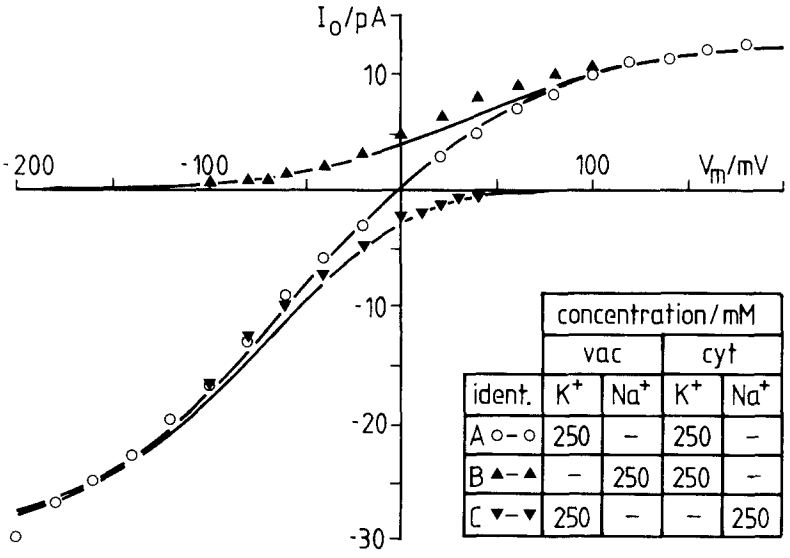

	concentration/mM			
	vac		cyt	
ident.	K^+	Na^+	K^+	Na^+
A o–o	250	–	250	–
B ▲–▲	–	250	250	–
C ▼–▼	250	–	–	250

Fig. 4. Current-voltage relationships of the open channel obtained from excised membrane patches; the control curve (data *A*) has been reproduced from Fig. 3*A*. K^+ has been totally replaced by Na^+ at the vacuolar side (*B*) or at the cytoplasmic side (*C*). Curves: fits of Eq. (10) to the data with the parameters of the 6-state model are given in Table 3

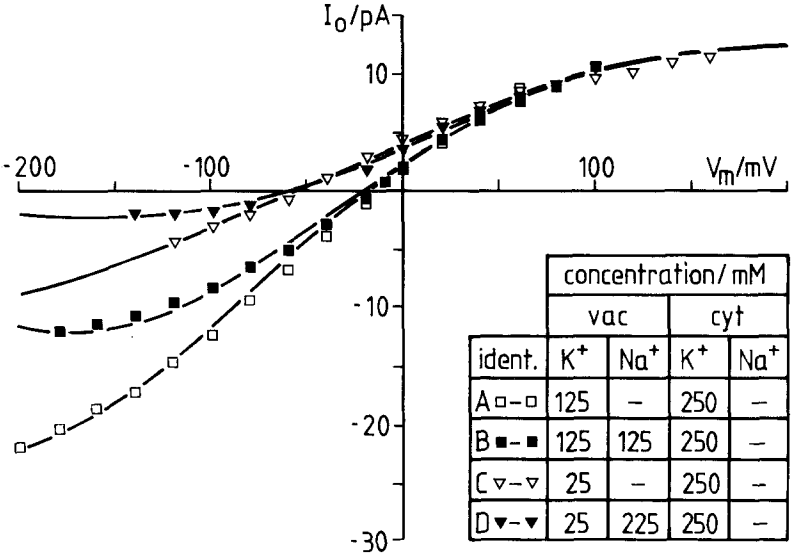

	concentration/mM			
	vac		cyt	
ident.	K^+	Na^+	K^+	Na^+
A □–□	125	–	250	–
B ■–■	125	125	250	–
C ▽–▽	25	–	250	–
D ▼–▼	25	225	250	–

Fig. 5. Effect of vacuolar Na^+ upon the current-voltage relationships of the open channel. Ionic conditions are as indicated in the inset; data (points) were obtained from four different experiments on excised membrane patches. The slight shift of the reversal voltages in the presenceof Na^+ is due to the decreased K^+ activities in higher salt concentrations. Curves: fits of Eq. (10) to the data with the parameters of the 6-state model are given in Table 3

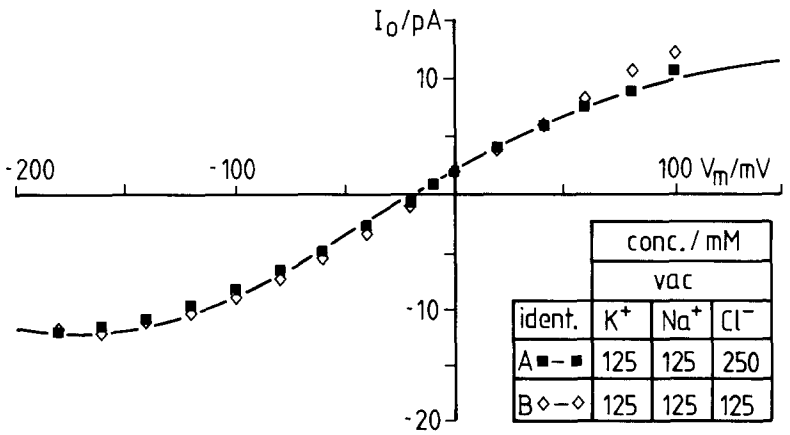

	conc./mM		
	vac		
ident.	K^+	Na^+	Cl^-
A ■–■	125	125	250
B ◇–◇	125	125	125

Fig. 6. Current-voltage relationships of the open channel. Cytoplasmic side: 250 mM KCl; vacuolar side: 125 mM KCl plus 125 mM Na^+. Na^+ has been added as NaCl (*A*) or as NaOH (*B*). pH in *B* has been adjusted by MES to pH 7.2, assuming the high MES concentration did not affect the channel currents. Curves: fits of Eq. (10) to the data with the parameters are given in Table 3

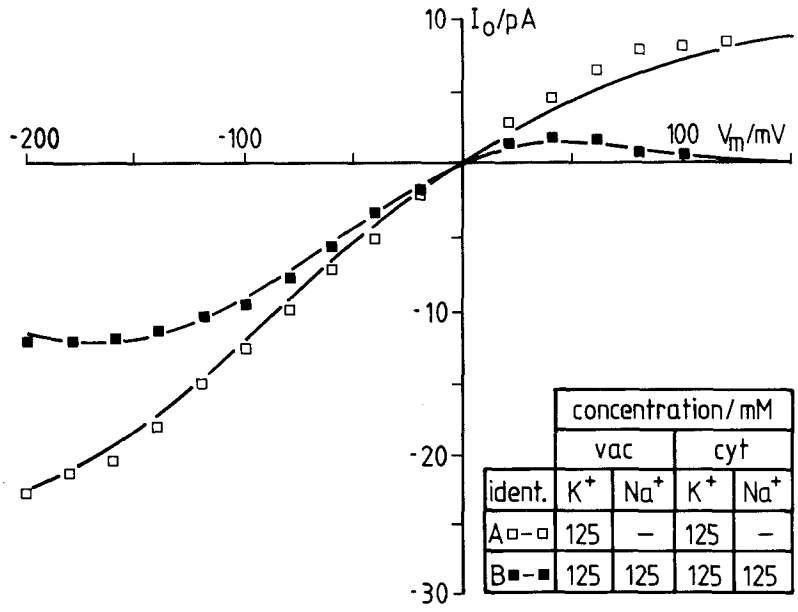

	concentration/mM			
	vac		cyt	
ident.	K^+	Na^+	K^+	Na^+
A□-□	125	–	125	–
B■-■	125	125	125	125

Fig. 7. Current-voltage relationships of the open channel in symmetric solutions (*see* inset). Note that the effect of Na^+ is more pronounced if added at the cytoplasmic side. Curves: fits of Eq. (10) to the data with the parameters are given in Table 3

KCl in both experiments. As the amplitude of the negative currents (i.e., K^+ currents directed from the vacuolar to the cytoplasmic side) was insensitive to the vacuolar Cl^- concentration, the inhibitory effect observed in the experiments of Fig. 5 has to be ascribed to the presence of Na^+ rather than to the increase of the vacuolar Cl^- concentration.

Figure 7 displays the current-voltage relationship of the open channel in symmetrical solutions with 125 mM KCl in (*A*) and with 125 mM KCl plus 125 mM NaCl in (*B*) on both sides of the membrane. As it can be seen from the data, the reduction of the positive K^+ currents in the presence of cytoplasmic Na^+ is more pronounced than that of the negative currents by vacuolar Na^+.

In Fig. 8, the ratio I_o'/I_o (a measure for the effect of Na^+ on the K^+ currents) is plotted *vs.* the actual membrane voltage on a log-linear scale. I_o' and I_o are the current amplitudes of the open channel in the presence and in the absence of Na^+, respectively. The points in Fig. 8, which are derived from the data of Fig. 7, demonstrate that the effect of Na^+ increases (I_o'/I_o decreases) with increasing voltage displacements of either sign.

Discussion

Membrane Identification

The vesicles used in this study exhibit ATP-driven current directed into the vesicles (Fig. 1) as well as ATP-induced internal acidification (*not shown*). This would also be possible with vesicles enclosed by inverse plasmalemma. However, the additional observation that all vesicles were colored red even in the absence of ATP, if prepared after staining the vacuole of the intact cell by neutral red, suggests the vesicles were enclosed by tonoplast in the right-side-out orientation and maintained a pH gradient during the isolation procedure.

The membrane current of 3.2 mA · m^{-2} as measured after addition of 1 mM Mg-ATP created a voltage across the tonoplast of about −7 mV (cytoplasmic side negative). This voltage corresponds well with the tonoplast voltage of −10 to −20 mV found in intact cells of *Chara corallina* (Findlay & Hope, 1964; Coster & Smith, 1977) and −4 mV as measured by Tester et al. (1987) using permeabilized cells of *Chara corallina*.

Selectivity

When K^+ has completely been replaced by Na^+ at either side of the membrane, as done in the experiments of Fig. 4, the single-channel currents directed from the *cis* side to the *trans* side (ought to be carried by Na^+) disappeared; the shape of the *I-V* characteristics flattened, but the saturation currents from the *trans* side to the *cis* side remained unaffected. Since no Na^+ currents appeared, no finite reversal voltage could be determined indicating the relative permeability $\alpha = P_{Na^+}/P_{K^+}$ being virtually zero.

From Table 1 it can be seen that under different KCl gradients (vacuolar KCl ranging from 2.5 to 250

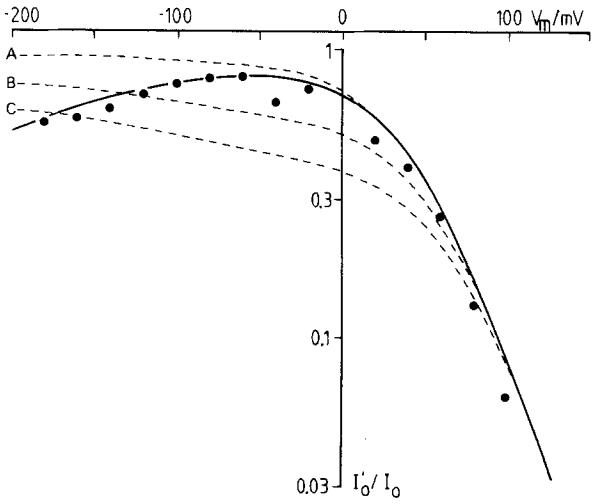

Fig. 8. Voltage dependence of the Na^+ effect expressed as the ratio I'_o/I_o (derived from the data of Fig. 7) plotted on a log-linear scale. I'_o and I_o represent the current amplitudes in the presence (Fig. 7*B*) and in the absence (Fig. 7*A*) of Na^+. The data are compared with the predictions of the 6-state model (Fig. 9*B*) with all parameters as listed in Table 3 (solid curve). The dashed curves represent the predictions of the model with voltage-insensitivity of the Na^+ binding/debinding outside (K_1) and all other parameters as in Table 3. K_1 was 1 (*A*), 10 (*B*) and 20 (*C*)

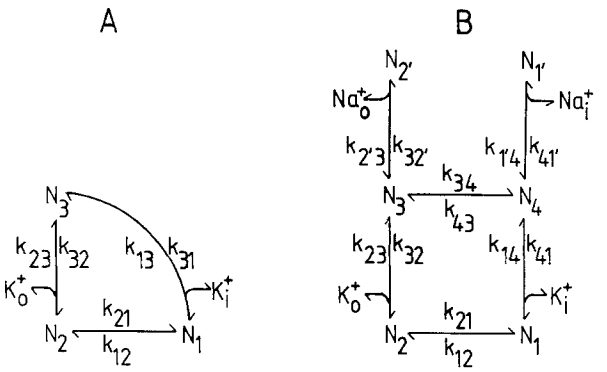

Fig. 9. Reaction-kinetic models and nomenclature. (*A*) 3-state model for the particular experimental situation when the substrate concentration has been changed outside. k_{12} and k_{21} designate the voltage-sensitive rate constants for the charge translocation. k_{32} is the rate constant for substrate (K^+) binding outside. (*B*) 6-state model for the *I-V* relationships of the K^+ channel considering the effect of Na^+ upon the K^+ currents. The rate constants k_{32} and k_{41} are the rate constants for the K^+ binding outside and inside, respectively. The equilibrium constants $K_1 = k_{32'}/k_{2'3}$ and $K_2 = k_{41'}/k_{1'4}$ describe the voltage-sensitive binding/debinding of Na^+ outside and inside, respectively. In the absence of Na^+ (K_1 and K_2 being zero) only states 1 to 4 remain, describing the K^+ uniport *per se*

mM, cytoplasmic KCl was 250 mM throughout) the experimentally determined reversal voltages were close to the respective equilibrium voltages for K^+ as calculated by the Nernst equation using K^+ activities. Therefore, the channel seems to be virtually impermeable to Cl^-, too.

Modeling

In this section, previous theoretical work of Hansen et al. (1981) and Gradmann, Klieber & Hansen (1987) is used, extended and applied.

The current-voltage analysis in the present paper focuses on cyclic models for K^+ uniport (Fig. 9) with the transporter being neutral and the substrate-transporter complex being positively charged. Such cyclic models consider a number of distinct states where N_i is the number of transporter molecules being in state i ($i = 1$ to n) and k_{ij} is the rate constant describing the transition from state i to state j.

For cyclic models with only one charge translocation step (Class I models), the current results from N_1 and N_2, which designate the amounts of transporters being in state 1 (charged binding site facing inside) and state 2 (charged binding site facing outside), respectively.

The transition rates, N_1k_{12} and N_2k_{21}, between these two states are voltage sensitive by

$$k_{12} = k_{12}^0 \exp\left(\frac{+zeV}{2kT}\right) \tag{1a}$$

$$k_{21} = k_{12}^0 \exp\left(\frac{-zeV}{2kT}\right) \tag{1b}$$

where k_{12}^0 and k_{21}^0 are the voltage-sensitive rate constants k_{12} and k_{21} at $V = 0$ mV, z is the valence of the charged particle crossing the membrane, e, k and T have their usual thermodynamic meaning and the factor 2 stands for the assumption of a symmetric Eyring barrier (Läuger & Stark, 1970).

The current-voltage equation for Class I models reads

$$I(V) = ze(k_{12}N_1 - k_{21}N_2). \tag{2}$$

The individual N_i can be calculated by solving a system of linear equations of the form

$$\frac{dN_i}{dt} = -N_i \sum_{j=1}^{n} k_{ij} + \sum_{j=1}^{n} (N_j k_{ji}) \tag{3}$$

with $dN_i/dt = 0$ for steady-state conditions.

The total number of transporters is

$$N = \sum_{i=1}^{n} N_i. \tag{4}$$

Table 2. Parameters of the 3-state model (Fig. 9*A*) for the current-voltage relationship of the open channel and its dependence on the external K^+ concentration[a]

Meaning	Parameter	Value
Translocation *i-o*	k_{12}^0	31.1
Translocation *o-i*	k_{21}^0	294.6
Debinding *o*	k_{23}	4865.9
Binding *o*	$\bar{k}_{32}$	794.2
Debinding *i* and reor. *i-o*	k_{13}	12.8
Binding *i* and reor. *o-i*	k_{31}	43.8

[a] Rate constants in 10^6 sec^{-1} (except for $\bar{k}_{32}$: 10^6 sec^{-1} M^{-1}): result of fit by the 3-state model to the experimental data in Fig. 3.

In the case of single-channel investigations, the total number of transporter molecules is $N = 1$ and the individual N_i is the probability of the transporter molecule being in state i and the rate constants k_{ij} have the meaning of transition probabilities.

The genuine model for the description of a single Class I *I-V* curve is the 2-state model.

A step-wide extension of this minimum model is mediated by additional data as measured under different experimental conditions. Changing the external substrate concentration, as done in the experiments of Fig. 3, yields a series of *I-V* relationships. Each of these *I-V* relationships can be used to determine the four parameters of the particular 2-state model. In order to describe the four data sets of Fig. 3 by an unique model, not only the voltage-dependent rate constants for the charge translocation step (k_{12} and k_{21}), but also the rate constants for external substrate binding/debinding (k_{32} and k_{23} in Fig. 9*A*) have to be treated separately since they are influenced by changing the external substrate concentration. Therefore, the appropriate model for the description of the four current-voltage relationships in Fig. 3 is a 3-state model (Fig. 9*A*) providing three pairs of rate constants, one of which is voltage sensitive.

For this 3-state model, the effective rate constant k_{32} has to be sensitive to the external substrate (K^+) concentration (activity):

$$k_{32} = \bar{k}_{32}[K]_o \tag{5}$$

where $\bar{k}_{32}$ is the fundamental rate constant for substrate (K^+) binding outside.

In order to examine whether the chosen 3-state model applies, the four data sets were used to a simultaneous fit in which five of the rate constants had to be common in all data sets and k_{32} was forced to be proportional to the external (vacuolar) substrate activity.

The curves fitted by the 3-state model with the numerical parameters as listed in Table 2 are virtually identical to the curves drawn in Fig. 3, which are the graphs of the fits of the 6-state model (Fig. 9*B*) discussed below.

Changing the substrate (K^+) concentration inside, too, as done in the experiment of Fig. 7A, yielded additional *I-V* relationships, which could be used to determine the parameters of a 4-state model (Fig. 9*B*, states 1 to 4).

In the 4-state model (Fig. 9*B*; states 1 to 4), the effective rate constants

$$k_{32} = \bar{k}_{32}[K^+]_o \tag{6a}$$

$$k_{41} = \bar{k}_{41}[K^+]_i \tag{6b}$$

depend on the respective substrate concentration, where $\bar{k}_{32}$ and $\bar{k}_{41}$ are the fundamental rate constants for substrate binding outside and inside, respectively.

It should be mentioned that due to the theory of model reduction (Gradmann et al., 1987) the numerical values of the 4-state model, (for example $\bar{k}_{32}$ of Eq. (6*a*)) are not identical with the corresponding values of the 3-state model ($\bar{k}_{32}$ in Eq. (5)).

For the 4-state model, the linear equation system Eq. (3) and Eq. (4) can be solved simultaneously, leading to the following expressions for N_1 and N_2

$$N_1 = \frac{X_1}{X_1 + X_2 + X_3 + X_4} \tag{7a}$$

and

$$N_2 = \frac{X_2}{X_1 + X_2 + X_3 + X_4} \tag{7b}$$

with the auxiliary expressions

$$X_1 = k_{32}k_{21}(k_{41} + k_{43}) + k_{34}k_{41}(k_{21} + k_{23}) \tag{8a}$$

$$X_2 = k_{41}k_{12}(k_{32} + k_{34}) + k_{43}k_{32}(k_{12} + k_{14}) \tag{8b}$$

$$X_3 = k_{23}k_{12}(k_{41} + k_{43}) + k_{43}k_{14}(k_{21} + k_{23}) \tag{8c}$$

$$X_4 = k_{14}k_{21}(k_{32} + k_{34}) + k_{34}k_{23}(k_{12} + k_{14}). \tag{8d}$$

Inserting Eqs. (7a) and (7b) into Eq. (2) gives the current-voltage equation for the 4-state model (Fig. 9*B*; states 1 to 4)

$$I(V) = ze\,\frac{k_{12}X_1 - k_{21}X_2}{X_1 + X_2 + X_3 + X_4}. \tag{9}$$

In the experiments of Figs. 4–7, not only the substrate (K^+) has been changed but another substrate (Na^+) has been added at one or both sides.

As shown by Figs. 5-7, Na^+ did affect the K^+ currents. Therefore, an interaction between Na^+ and the transporter molecule has to take place at both sides, which can be taken into account by the extension of the 4-state model to a 6-state model (Fig. 9*B*) with the two equilibrium constants $K_1 = k_{32'}/k_{2'3}$ and $K_2 = k_{41'}/k_{1'4}$, describing the Na^+ binding/debinding outside and inside, respectively. Transitions between states 1′ and 2′, which would describe the translocation of Na^+, are not allowed in this model since the channel is impermeable to Na^+ (Fig. 4).

For this 6-state model the current-voltage equation reads

$$I(V) = ze \frac{k_{12}X_1 - k_{21}X_2}{X_1 + X_2 + (1 + K_1)X_3 + (1 + K_2)X_4}. \quad (10)$$

The voltage sensitivity of the Na^+ effect (Fig. 7) is accounted for, when the two equilibrium constants K_1 and K_2 become voltage sensitive, so that

$$\frac{k_{32'}}{k_{2'3}} = K_1 = \bar{K}_1^0[Na^+]_o \exp\left(\frac{-z_1 eV}{kT}\right) \quad (11a)$$

$$\frac{k_{41'}}{k_{1'4}} = K_2 = \bar{K}_2^0[Na^+]_i \exp\left(\frac{+z_2 eV}{kT}\right) \quad (11b)$$

with K_1^0 and K_2^0 being the respective voltage-sensitive equilibrium constants for Na^+ binding/debinding at $V = 0$ mV, z_1 and z_2 are the effective charge numbers describing the voltage sensitivity of the respective equilibrium constant.

One set of 12 parameters (the eight rate constants of the K^+ loop, the two equilibrium constants $\bar{K}_1^0$ and $\bar{K}_2^0$ as well as the effective charge numbers z_1 and z_2) were fitted by Eq. (10) to the entire ensemble of the experimental data in Figs. 3–7. The resulting numerical values of these 12 parameters are listed in Table 3. The curves in Figs. 3–7 are the graphical representation of this simultaneous fit. In that fit the rate constants k_{32}, k_{41} (rate constants for the K^+ bindings) and the equilibrium constants K_1^0 and K_2^0 (equilibrium constants for Na^+ binding/debinding at the respective side at $V = 0$ mV) were forced to vary with the respective substrate activities, while all other rate constants had to be in common for all ten data sets.

As all ten data sets correspond well with the fitted curves, the chosen 6-state model seems to satisfy the experimental data. When no Na^+ is present at either side of the membrane, K_1 and K_2, (Eqs. (11a) and (11b)) in the 6-state model become zero. The model for the description of the K^+ transport *per se* (without Na^+ added) is the 4-state model (states 1 to 4 in Fig. 9*B*), the numerical values of the eight rate constants of which are identical to the parameters of the 6-state model (Table 3) with $K_1 = K_2 = 0$.

Table 3. Parameters of the 6-state model (Fig. 9*B*) for the current-voltage relationships of the open channel considering the effect of Na^+ upon the K^+ currents[a]

Meaning	Parameter	Value
K^+ translocation *i-o*	k_{12}^0	2031.6
K^+ translocation *o-i*	k_{21}^0	420.7
K^+ debinding *o*	k_{23}	8422.8
K^+ binding *o*	$\bar{k}_{32}$	1057.1
Empty site reorient. *o-i*	k_{34}	18.1
Empty site reorient. *i-o*	k_{43}	39.9
K^+ binding *i*	$\bar{k}_{41}$	785.7
K^+ debinding *i*	k_{14}	12600.3
Na^+ binding/debinding *o*	$\bar{K}_1^0$	1.1
Na^+ binding/debinding *i*	$\bar{K}_2^0$	8.9
Effective charge number (Na_o^+)	z_1	0.4
Effective charge number (Na_i^+)	z_2	1.0

[a] Rate constants in 10^6 sec^{-1} (except for $\bar{k}_{32}$, $\bar{k}_{41}$: 10^6 sec^{-1} M^{-1}); equilibrium constants $\bar{K}_1^0$ and $\bar{K}_2^0$ in M^{-1}; result of fit by Eq. (11) to all experimental data of Figs. 3–7.

With the equilibrium constants K_1 and K_2 being voltage insensitive, the effect of Na^+ on the K^+ currents cannot be described satisfactorily. This is shown in Fig. 8, where the effect of Na^+ (I_o'/I_o) derived from the data in Fig. 7 is compared with the intrinsic effect of the 6-state model with the parameters as in Table 3 (solid curve) and several *voltage-independent* equilibrium constants K_1 (dashed curves). In the negative voltage range, only the solid curve (with K_1 being *voltage sensitive*) shows the increasing effect of Na^+ with increasing negative voltages. In the dashed curves (*A-C*, with voltage independent $\bar{K}_1$, ranging from 1 to 20) the effect of Na^+ decreases with increasing negative voltages, which is in contrast to the experimental data.

Alternative Models

The model used in the present paper can be understood as a special case of the 6-state model presented by Gradmann et al. (1987) for the quantitative analysis of current-voltage data from an open K^+ channel with a finite permeability to Na^+ as well ($k_{1'2'}, k_{2'1'} > 0$). As the data in the present study demonstrate that Na^+ is not transported through the channel, the Na^+ loop in the 6-state model (used by Gradmann et al., 1987) has to be interrupted between states 2′ and 1′, i.e., $k_{2'1'}$ and $k_{1'2'}$ has to be zero. The voltage sensitivity of the effect of Na^+ on the K^+ currents requires the equilibrium constants K_1 and K_2 to be voltage sensitive. The equilibrium constants K_1 and K_2 can be understood as a lumped

reaction describing the Na^+ binding/debinding and the voltage-dependent hold of Na^+ on the K^+-binding site.

Recently, Laver and Walker (1987) applied the theory of diffusion-limited ion flow through pores (Läuger, 1976) to the K^+ channel in the membrane of cytoplasmic droplets of *Chara*.

This model predicts some fundamental features, which are characteristic for the K^+ channel investigated in the present study, as well:

> The current-voltage characteristic of a diffusion-limited channel is strongly saturating.
>
> Addition of an impermeable electrolyte decreases the saturation current.

However, other characteristics of this model are inconsistent with the properties of the K^+ channel measured in the present study.

> The saturation currents of a diffusion-limited channel are proportional to the substrate concentration.

The data in Fig. 3 clearly show that the saturation currents are not proportional to the substrate concentration in the charge-delivering compartment. For the K^+ channel in the membrane of cytoplasmic droplets of *Chara corallina*, a similar subproportional dependence measured in solutions with K^+ concentrations ranging from 77 to 200 mM (without Na^+ added) has been observed by Lühring (1986).

> Diffusion limitation predicts, that in the limit of infinite intrinsic permeability of the channel, the ratio I_o'/I_o becomes at least 0.5 for large voltages (I_o' represents the current in the presence, I_o that in the absence of an excess of inert electrolyte).

However, the data in Fig. 8 show a voltage-dependent decrease of the ratio I_o'/I_o clearly below 0.5 for high positive voltages.

> The current-voltage characteristic of a diffusion-limited channel cannot display regions of negative slope conductance.

Negative slope conductance is clear in the data of Fig. 7*B* for positive membrane voltages. Negative slope conductance at positive membrane voltages can also be seen in the data reported by Lühring (1986) for the membrane of cytoplasmic droplets of *Chara corallina*.

Comparisons

The similarities (high selectivity for K^+, saturation characteristics, asymmetry, inhibition by Na^+) of the predominant K^+ channel from the tonoplast of *Chara corallina* described here with the predominant K^+ channel from cytoplasmic droplets of *Chara corallina* (Lühring, 1986) confirms the conclusion of Lühring (1986) about the tonoplast origin of the channel in the outer membrane of cytoplasmic droplets.

It is tempting to point out some similarities between the macroscopic *I-V* curves of the tonoplast from permeabilized cells of *Chara corallina* (Tester et al., 1987) and the microscopic *I-V* characteristics of its predominant (K^+) channel described here, especially with respect to the common phenomenon of negative slope conductance at large voltage displacements from the equilibrium. In the macroscopic *I-V* characteristics of the tonoplast, regions of negative slope conductance appear at high Cl^- concentrations (Tester et al., 1987), while the data in the present study show the development of negative slope conductance in the microscopic *I-V* characteristics of the single open K^+ channel in the presence of Na^+. In macroscopic channel currents, however, the phenomenon of negative slope conductance can also arise by a voltage-dependent increase of the mean closed time of the channel, while the microscopic *I-V* characteristic of the open channel maintains a positive slope conductance over the entire voltage range (Bertl & Gradmann, 1987; Bertl, Klieber & Gradmann, 1988).

Conclusions

The predominant ion channel in the tonoplast of *Chara corallina* is highly specific to K^+ and impermeable to Na^+ and Cl^-. Although Na^+ is not transported through the channel, the K^+ currents are affected by Na^+. The presence of Na^+ at either side of the membrane inhibits the K^+ currents directed from the *cis* side to the *trans* side at last leading to regions of negative slope conductance (Fig. 7*B*).

In order to describe the *I-V* relationship of the K^+ channel in the presence of a second cation (Na^+), which does affect the K^+ currents but is not transported through the channel, a 6-state model has been suggested to be appropriate. This model consists of a cyclic 4-state model for the K^+ uniport, the empty binding sites of which equilibrate with two additional states (2′ and 1′) via the two voltage-sensitive equilibrium constants K_1 and K_2.

The author thanks D. Gradmann and H.G. Klieber for many hours of valuable discussions and for critical reading of the manuscript. This work was supported by the Deutsche Forschungsgemeinschaft (Gr 409/9-5,6).

References

Beilby, M.J. 1985. Potassium channels at *Chara* plasmalemma. *J. Exp. Bot.* **36**:228–239

Bertl, A., Gradmann, D. 1987. Current-voltage relationships of potassium channels in the plasmalemma of *Acetabularia*. *J. Membrane Biol.* **99:**41–49

Bertl, A., Klieber, H.G., Gradmann, D. 1988. Slow kinetics of a potassium channel in *Acetabularia*. *J. Membrane Biol.* **102:**141–152

Coster, H.G.L., Smith, J.R. 1977. Low-frequency impedance of *Chara corallina:* Simultaneous measurements of the separate plasmalemma and tonoplast capacitance and conductance. *Aust. J. Plant Physiol.* **4:**667–674

Coyaud, L., Kurkdjian, A., Kado, R., Hedrich, R. 1987. Ion channels and ATP-driven pumps involved in ion transport across the tonoplast of sugar beet vacuoles. *Biochim. Biophys. Acta* **902:**263–268

Findlay, G.P., Hope, A.B. 1964. Ionic relations of cells of *Chara australis* VII. The separate electrical characteristics of the plasmalemma and tonoplast. *Aust. J. Biol. Sci.* **17:**62–77

Gradmann, D., Klieber, H.G., Hansen, U.P. 1987. Reaction kinetic parameters for ion transport from steady state current-voltage curves. *Biophys. J.* **51:**569–585

Hamill, O.P., Marty, A., Neher, E., Sakmann, B., Sigworth, F.J. 1981. Improved patch-clamp techniques for high resolution current recording from cells and cell-free membrane patches. *Pfluegers Arch.* **391:**85–100

Hansen, U.P., Gradmann, D., Sanders, D., Slayman, C.L. 1981. Interpretation of current-voltage relationships for "active" ion transport systems: I. Steady-state reaction-kinetic analysis of Class-I mechanisms. *J. Membrane Biol.* **63:**165–190

Hedrich, R., Barbier-Brygoo, H., Felle, H., Flügge, U.I., Lüttge, U., Maathuis, F.J.M., Marx, S., Prins, H.B.A., Raschke, K., Schnabl, H., Schroeder, J.I., Struve, I., Taiz, L., Ziegler, P. 1988. General mechanisms for solute transport across the tonoplast of plant vacuoles: A patch-clamp survey of ion channels and proton pumps. *Botan. Acta* **1:**7–13

Hedrich, R., Flügge, U.I., Fernandez, J.M. 1986. Patch-clamp studies of ion transport in isolated plant vacuoles. *FEBS Lett.* **204:**228–232

Hedrich, R., Neher, E. 1987. Regulation of voltage-dependent ion channels in plant vacuoles by cytoplasmic calcium. *Nature (London)* **329:**834–836

Homble, F., Ferrier, J.M., Dainty, J. 1987. Voltage-dependent K^+-channel in protoplasmic droplets of *Chara corallina*. A single channel patch clamp study. *Plant Physiol.* **83:**53–57

Hope, A.B., Walker, N.A. 1975. The Physiology of Giant Algal Cells. Cambridge University Press, London

Läuger, P. 1976. Diffusion-limited ion flow through pores. *Biochim. Biophys. Acta* **455:**493–509

Läuger, P., Stark, G. 1970. Kinetics of carrier-mediated transport across lipid bilayer membranes. *Biochim. Biophys. Acta* **211:**458–466

Laver, D.R., Walker, N.A. 1987. Steady state voltage-dependent gating and conduction kinetics of single K^+ channels in the membrane of cytoplasmic drops of *Chara australis*. *J. Membrane Biol.* **100:**31–42

Lühring, H. 1986. Recording of single K^+ channels in the membrane of cytoplasmic drop of *Chara australis*. *Protoplasma* **133:**19–28

Moriyasu, Y., Shimmen, T., Tazawa, M. 1984. Electrical characteristics of the vacuolar membrane of *Chara* in relation to pH_v regulation. *Cell Struct. Funct.* **9:**235–246

Reeves, M., Shimmen, T., Tazawa, M. 1985. Ionic activity gradients across the surface membrane of cytoplasmic droplets prepared from *Chara australis*. *Plant Cell Physiol.* **26:**1185–1193

Sakano, K., Tazawa, M. 1986. Tonoplast origin of the envelope membrane of cytoplasmic droplets prepared from *Chara* internodal cells. *Protoplasma* **113:**247–249

Sakmann, B., Neher, E. 1983. Single-Channel Recording. Plenum, New York

Shimmen, T., Tazawa, M. 1983. Control of cytoplasmic streaming by ATP, Mg^{2+} and cytochalasin B in permeabilized *Characeae* cell. *Protoplasma* **115:**18–24

Svintitskikh, V.A., Andrionov, V.K., Bulychev, A.A. 1985. Photo-induced H^+ transport between chloroplasts and the cytoplasm in a protoplasmic droplet of *Characeae*. *J. Exp. Bot.* **36:**1414–1429

Tazawa, M., Kikuyama, M., Shimmen, T. 1976. Electrical characteristics and cytoplasmic streaming of *Characeae* cells lacking tonoplast. *Cell Struct. Funct.* **1:**167–176

Tester, M., Beilby, M., Shimmen, T. 1987. Electrical characteristics of the tonoplast of *Chara corallina:* A study using permeabilised cells. *Plant Cell Physiol.* **28:**1555–1568

Received 12 August 1988; revised 11 January 1989